JOURNAL OF OPTOELECTRONICS AND ADVANCED MATERIALS, Vol. 11, No. 8, August 2009, p. 1082 - 1087

Effect of annealing below crystallization temperature on structural and mechanical properties of $Co_{66}Si_{16}B_{12}Fe_4Mo_2$ metallic glass

P. KUMAR, K. SINGH*, T. P. YADAV, O. N. SRIVASTAVA
Department of Physics, Faculty of Science, Banaras Hindu University, Varanasi – 221005 India.

The influence of thermal treatment on the structural and mechanical properties of $Co_{66}Si_{16}B_{12}Fe_4Mo_2$ metallic glass has been investigated in present study. $Co_{66}Si_{16}B_{12}Fe_4Mo_2$ metallic glass has been subjected to isothermal annealing at 450^0C for different time such as 1, 2, 5 and 8 h and studied by X-ray diffraction and scanning electron microscopy techniques. The Voight function analysis has been used for calculation of effective crystallite size and relative strain of all the annealed samples. The crystallite size has been found to be ~ 40 – 60 nm after different h of annealing. The mechanical properties of above alloy before and after annealing has been studied by micro-hardness technique. Sample annealed for 8 h at 450^0C becomes completely crystallized due to local structural rearrangements of the amorphous matrix by promoting the retention of nucleation during annealing and shows the maximum hardness among all crystalline and glassy samples.

(Received February 24, 2009; accepted August 05, 2009)

Keywords: Metallic glass, Co-Si-B-Fe-Mo annealing, Crystallization

1. Introduction

Metallic glasses represent a class of materials that combine a metallic electronic structure with amorphous (non-crystalline) molecular structure lacking the long-range crystalline order of conventional alloys. They are prepared by rapid solidification of alloy melts, in which cooling rate of 10^6 Ks^{-1} prevent the nucleation and subsequent growth of a crystalline phase [1]. The rapid quenching process used for the production of the amorphous alloys yields a solid ribbon of about 20–60 μm thickness and 1–25 mm width [2, 3]. Metal–metalloid glasses and metal–metal glasses are two broad categories of glassy alloys. Metal-metalloid glasses are the most widely studied group, with a metal to metalloid ratio of 4:1 being typical. This consistent glass forming ratio suggests that a specific type of chemical bonding is present, it has been found that alloy compositions that form ‘‘deep eutectics’’ in the phase diagram generally display the greatest ease of amorphisation. The metalloid elements are believed to stabilize the amorphous structure by providing an appropriate atomic volume. Owing to their disorderness or amorphous structure, metallic glasses possess some excellent properties such as high hardness, tensile strength, magnetic permeability, electrical resistivity along with resistance to gamma radiation damage and corrosion [4]. A combination of these properties of metallic glasses makes them attractive for various technological applications. The tribological properties of metallic glasses has also been studied because of their potential applications as audio/video recording heads, foil bearings, electric razors and razor blades [5, 6]. Several studies reported that metallic glasses have higher sliding friction and wear resistance than its crystallized state [7-14]. To the contrary, there are also reports indicating that the wear performances of metallic glass are significantly inferior to the annealed state and traditional crystalline alloy [15, 16]. Among the recently developed metallic glass systems, Co-based alloys exhibit the excellent soft magnetic properties with near to zero magnetostriction, which renders the material a potential candidate for a variety of industrial applications, including magnetic recording heads and electronic security sensors [17-19]. Gradually devitrified $Co_{66}Si_{16}B_{12}Fe_4Mo_2$ metallic glasses is known as VITROVAC 6025 [20]. Even at the initial stages of crystallization, the coexistence of different magnetic phases, and the possibility of modifying their size distribution and relative volume fraction through annealing makes these materials good environments to investigate interactions among magnetic particles, surface effects, transport properties and several other new phenomenon that emerge with the reduced dimensions of crystallites [21, 22]. Internal stresses are always present in as-prepared metallic glasses, they arise from inhomogeneities due to different cooling rates during quenching. However the amorphous microstructure, allows atomic rearrangements to occur at moderate temperatures, lower than crystallization temperature. Annealing is the usual way to induce the structural relaxation, which relaxes the internal stresses [23]. Heat treatments may induce structural change in metallic, if they are subjected to heat treatments and one can obtain micro/nanocrystalline phases after suitable thermal treatments at temperatures below or above the crystallization temperature. Research into the mechanical response of metallic glasses dates back to the 1960s when it was demonstrated that thin ribbons, wires or sheets of metals in an amorphous or in glassy state could be produced at very high cooling rates (over 10^5 K s^{-1}) [1]. Since these metallic glasses could be produced in bulk form, the mechanical properties of the amorphous alloys

became topics of considerable research for possible structural applications. Indentation test has recently been used to examine mechanical properties of metallic glasses. There are several reports regarding to the measurements of mechanical properties by indentation technique on different metallic glasses [24-28]. Present study aims to investigate the nucleation and growth mechanism during annealing below the crystallization temperature of $Co_{66}Si_{16}B_{12}Fe_4Mo_2$ metallic glass ribbon. In addition, the influence of annealing time and temperature on the mechanical behaviour were also studied.

2. Experimental techniques

The material investigated in present study is an as-cast, fully amorphous, $Co_{66}Si_{16}B_{12}Fe_4Mo_2$ metallic glass ribbon (trade name VITROVAC 6025 nominal compositions in at. wt %) obtained by melt spinning technique. $Co_{66}Si_{16}B_{12}Fe_4Mo_2$ samples were subjected to isothermal annealing (below crystallization temp 550^0C) at 450^0C for different time so as to produce a series of samples with gradually coarser nanostructure. Four pieces of the amorphous sample were cut in the form of square (dim 5 X 5 mm) and were annealed at 450^0C for different time 1, 2, 5 and 8 h. The annealing of the samples was carried out in a conventional electric tube furnace, to prevent eventual surface oxidation all samples were situated in evacuated quartz ampoules. As cast and heat-treated samples was characterized by powder X-ray diffraction (Philips1710 X-ray diffractometer) with Cu-Kα radiation. The effective crystallite size and relative strain of heat-treated products were calculated based on line broadening of XRD peaks. The use of the Voight function for the analysis of the integral breadths of broadened X-ray diffraction line profiles forms the basis of a rapid and powerful single line method of crystallite-size and strain determination. In this case the constituent Cauchy and Gaussian components can be obtained from the ratio of full width at half maximum intensity (2ω) and integral breadth (β) [29-30]. In a single line analysis, the apparent crystallite size ' D ` and strain 'e ` can be related to Cauchy (β_c) and Gaussian (β_G) widths of the diffraction peak at the Bragg angle θ;

$$D = \lambda / \beta_c \cos\theta \quad (1)$$

and

$$e = \beta_G / 4 \tan\theta \quad (2)$$

The constituent Cauchy and Gaussian components can be written as

$$\beta_c = (a_0 + a_1\psi + a_2\psi^2)\,\beta$$

$$\beta_G = (b_0 + b_{1/2}(\psi - 2/\pi)^{1/2} + b_1\psi + b_2\psi^2)\,\beta$$

where a_0, a_1 & a_2 are Cauchy constants.

b_0, $b_{1/2}$, b_1 & b_2 are Gaussian constants.

and $\psi = 2\omega/\beta$ where β is the integral breadth obtained from XRD peak.

$a_0 = 2.0207$, $a_1 = -0.4803$, $a_2 = -1.7756$

$b_0 = 0.6420$, $b_{1/2} = 1.4187$, $b_{1=} - 2.2043$,

$b_2 = 1.8706$

The values of Cauchy and Gaussian constant have been taken from the table of Langford [29].

From these, we have calculated the crystallite size D and the lattice strain "e" for the annealed alloys. The microstructures of as prepared and annealed samples were inspected by Scanning Electron Microscopy (SEM) Philips XL-20 observations made operating at 30 keV. The micro-hardness measurement was carried out by Vickers Micro-hardness Tester by indentation technique several times at six different loads as 50, 100, 200, 300, 500, 1000 g on well polished cross-section of each sample.

3. Results and discussion

3.1. Structural studies

The X-ray diffraction (XRD) pattern for the $Co_{66}Si_{16}B_{12}Fe_4Mo_2$ alloy obtained after melt spun ribbon is shown in Fig. 1. A diffuse broad peak appears indicating the formation of the amorphous phase (Fig.1). XRD pattern clearly indicates that at the initial there was no presence of any crystalline or nanocrystalline phase in melt spun ribbon. To study the effect of annealing on the melt spun amorphous ribbon were subjected to annealing for various time periods. XRD patterns obtained followed by annealing at 450^oC for 1, 2 and 5 h respectively has given in Fig. 2 (a), (b) and (c). The XRD patterns corresponding to 2 and 5 h annealed samples (Fig.2 (b, c)) have been indexed as Co_2 (B, Fe) type hexagonal structure with a = 5.0 Å and c = 4.1 Å. The formation of the nanocrystalline phase due to the subsequent annealing blew crystallization temperature has been observed for the first time in $Co_{66}Si_{16}B_{12}Fe_4Mo_2$ alloy.

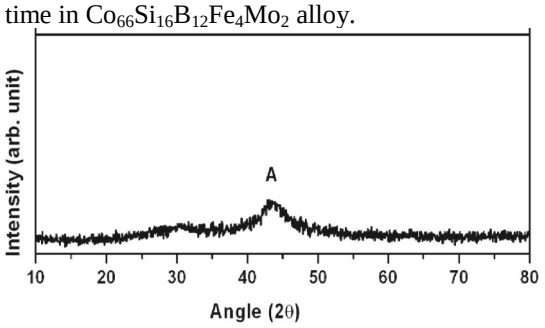

Fig. 1. X-ray diffraction pattern of as prepared amorphous sample.

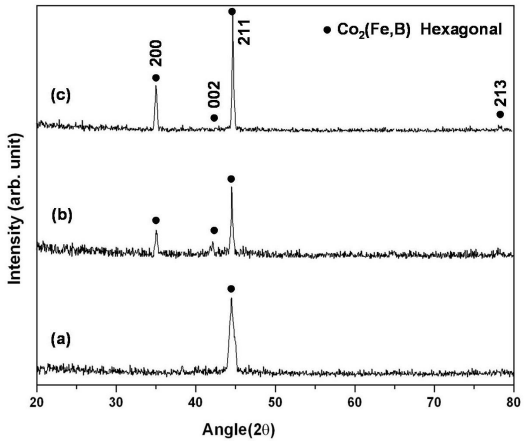

Fig. 2. XRD of 1 h (a), 2 h (b) and 5 h (c) annealed sample.

Fig. 3 (a) represents the morphology of as cast melt spun amorphous alloy. Very small crystallites with very low volume concentration are formed in the sample after 1 h annealing as shown in Fig. 3(b). However, it is noteworthy that the morphology of the growing crystals is quite complex, suggesting simultaneous occurrence of two crystalline phases which may be due to that the first stage of crystallization is of eutectic type. Increasing annealing time up to 8 h, leads to total crystallization of the sample Fig. 3(e). A further increase of the annealing time leads to comparatively bigger nanocrystalline occupying the whole volume of the sample. The average crystallite size for all samples is ranging from 40 nm to 60 nm. Optical micrograph showing an impression from indentation is shown in Fig.4 [A-E]. Fig 4(A) clarifying that the features around the indent are not cracks but overlapping layers of displaced material as a result of indenter. It may indicate the improvement of the toughness of this type of materials. The absence of shear bands around the indention suggests that the formation is supported by the nanophase of the alloy. Vickers hardness values for all samples are shown in Fig. 5. The hardness of the annealed samples increases exponentially with annealing time Fig. 6. We observe a drastic increment of five orders of magnitude in hardness of nanocrystalline phase of 8 h annealed sample as compared to as prepared glassy alloy. It confirms our expectations that nanocrystalline phase is much harder as compared to amorphous state. Hardness in both glassy and crystalline materials is expected to be different due to their structural difference.

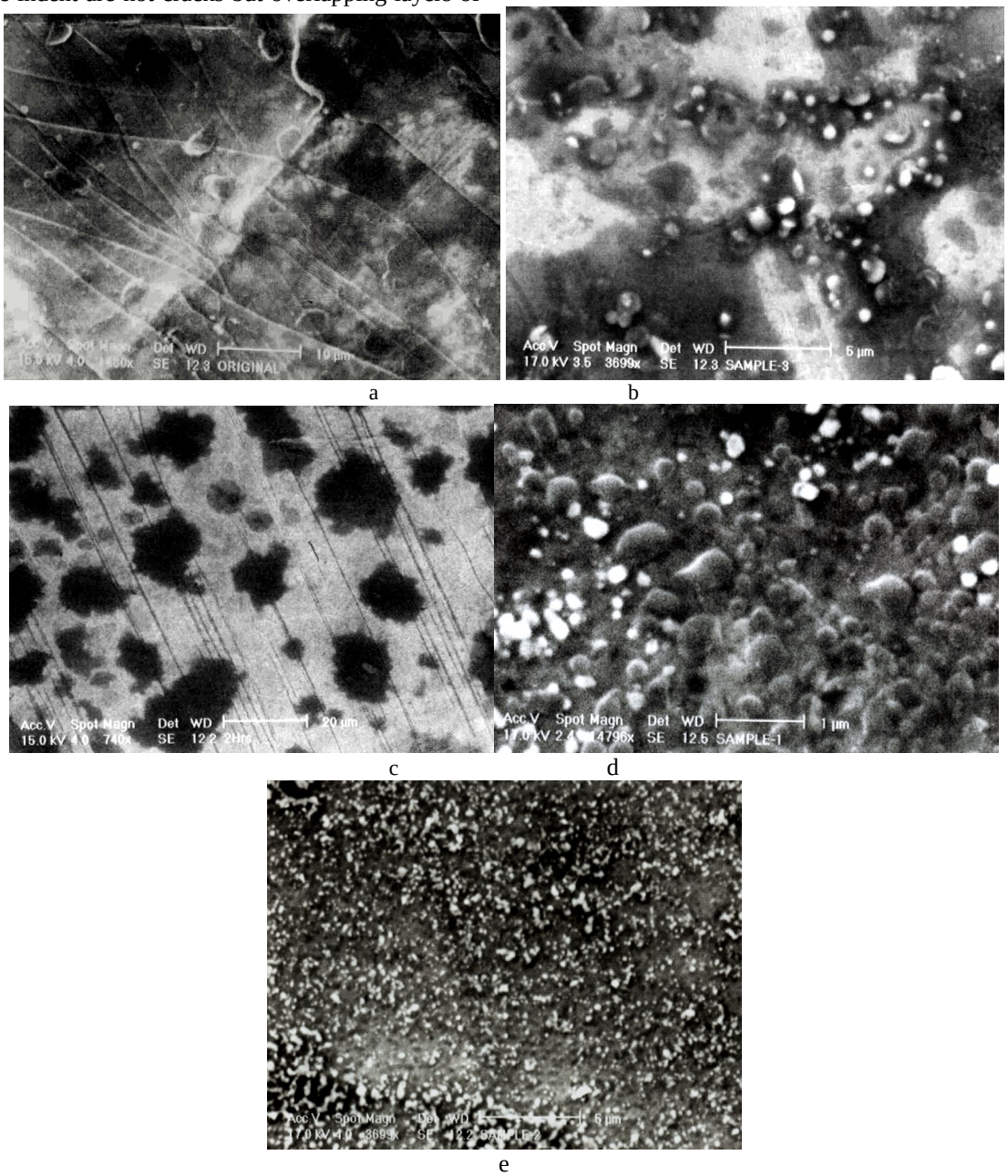

Fig. 3. SEM micrographs of as prepared (A), 1 h (B), 2h (C), 5 h (d) and 8 h (E) annealed sample at 450^0C.

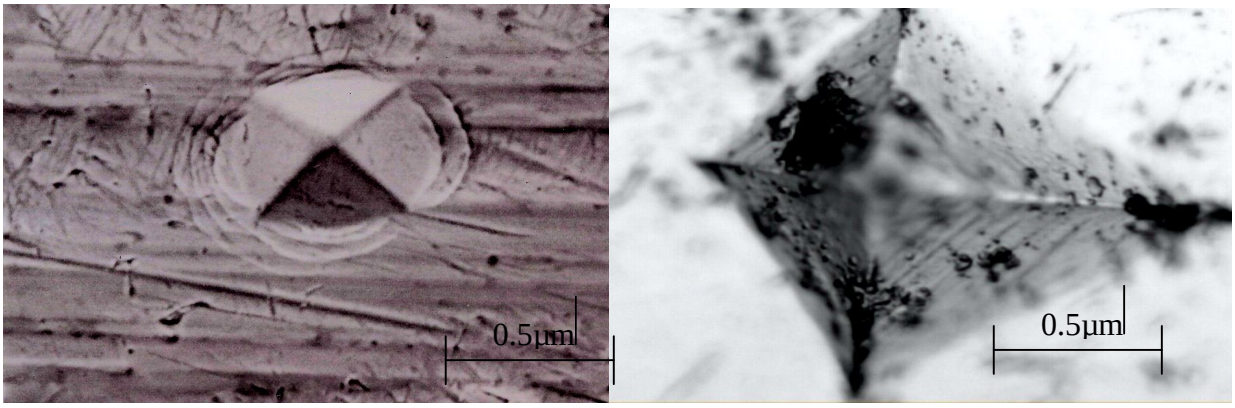

a b

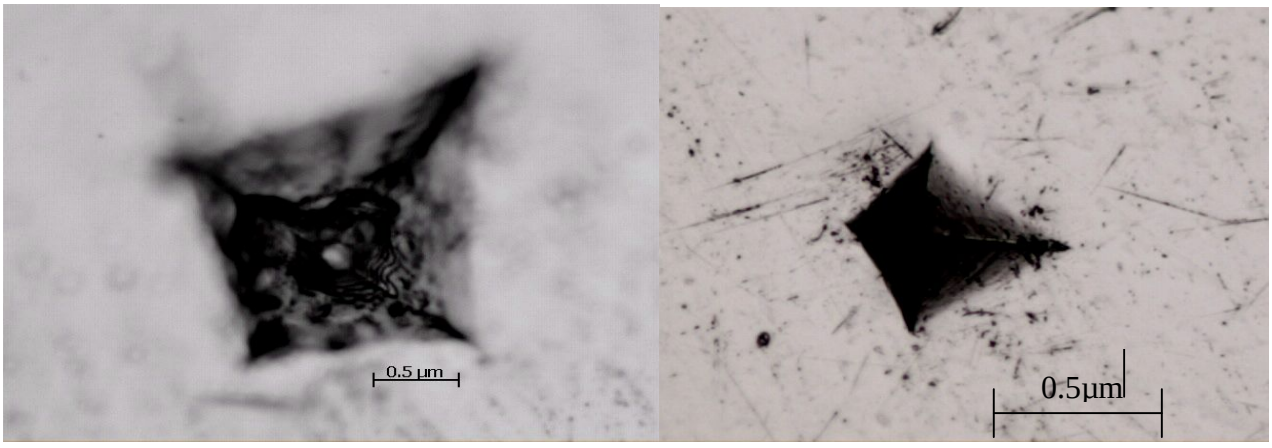

c d

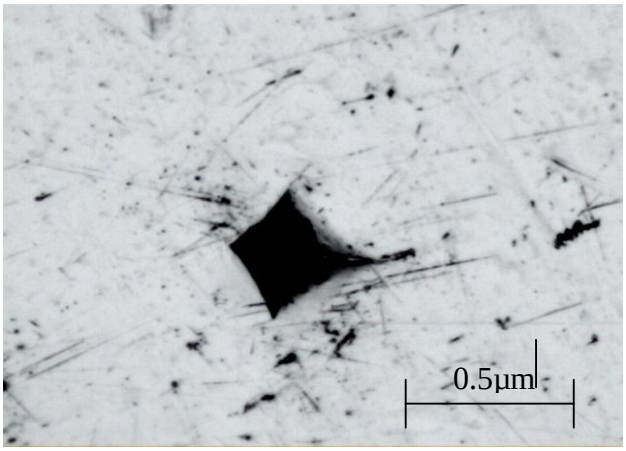

e

Fig. 4. Optical micrographs of as cast (A), 1 h (B), 2 h (C), 5 h (D) and 8 h (E) annealed sample at 450^{0}C at the load of 100 g.

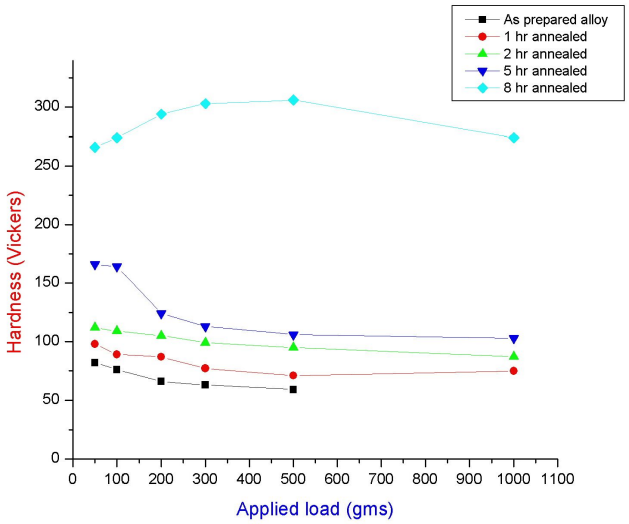

Fig. 5. Variation of Vickers hardness of all samples at different applied loads.

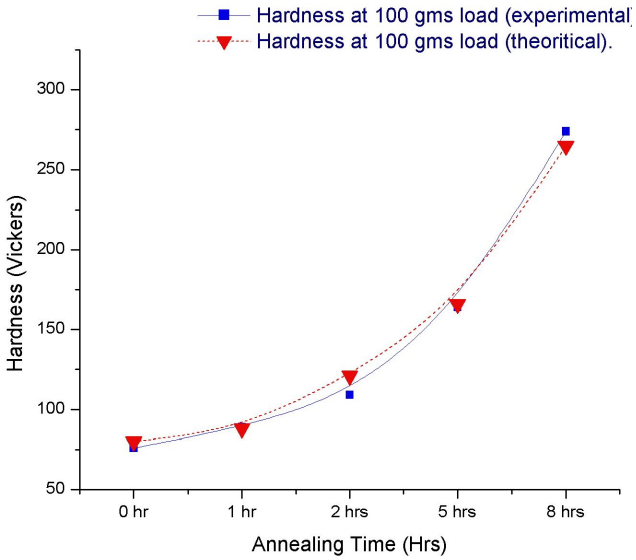

Fig. 6. Experimental and theoretical variation of hardness as a function of annealing time at the load of 100 g.

3.2. Hardness measurements

It is observed that the hardness of as prepared and annealed samples follows the behaviour as given by the equation:

$$H = H_0 \exp(kt) \qquad (3)$$

Where **H** is the hardness of the sample at different weights $\mathbf{H_0}$ is the hardness of the as prepared sample (different for different weights), **k** is some hardness constant and **t** is annealing time (in h). Plotting of experimental and theoretical values of hardness with respect to annealing time at the load of 100 g and all other values, follow the same pattern (Fig.6). The mechanical properties of $Co_{66}Si_{16}B_{12}Fe_4Mo_2$ metallic glasses at different annealing time have not been studied previously. The annealing can effectively enhance the hardness due to the dispersion of hard particles within the amorphous matrix. There are reports suggesting that a proper amount of nanocrystals embedded in the amorphous matrix could increase mechanical strength such as fracture stress and could impede crack propagation [31, 32]. Sample annealed for 8 h at 450^0 C becomes completely crystallized and shows the excellent hardness properties among all crystalline and as prepared amorphous samples.

4. Conclusions

The isothermal annealing of $Co_{66}Si_{16}B_{12}Fe_4Mo_2$ amorphous ribbons sample results in nanocrystalline structures. It is observed from SEM micrograph of sample annealed at 450^0C for 8 h, it becomes completely crystalline occupying the whole volume of the sample. Hardness increases exponentially, five orders of magnitude from as cast to 8 h annealed sample. The annealing conditions used in the present study have led to nanocrystals, which are smaller than the usual shear band sizes in bulk amorphous alloys and hence they are able to disrupt shear-band propagation, which has possibly resulted in a higher hardness on crystallization. This is an interesting feature and may throw light on the behaviour in nanophase materials.

Acknowledgements

Pushpendra Kumar is grateful for support from the University Grant Commission New Delhi for providing financial assistance under Rajeev Gandhi National Fellowship Scheme (RGNFS). We are also thankful to Prof. N.S. Saxena for fruitful discussion and providing help in various ways.

References

[1] W.Clement, R.H. Willens, P. Duwez, Nature **187,** 869, (1960).
[2] H.S. Chen, Acta metall. **22,** 1505, (1974).
[3] H.S. Chen, Rep. Prog. Phys. **43,** 353 (1980).
[4] F.E. Lubrosky (Ed.), Amorphous Metallic Alloys, Butterworths Monographs in Materials, (1983).
[5] T. Masumoto, Proceedings of the 4th International Conference on Rapidly Quenched Metals, Sendai, Japan, 5, (1981).
[6] F.H. Froes, R. Carbonara, J. Met. **40,** 20, (1988).
[7] K. Miyoshi, ASLE Trans. **27** (4), 295, (1983).
[8] R. Klinger, H.G. Feller, Wear **86,** 287, (1983).
[9] R. Moreton, J.K. Lancaster, J. Mater. Sci. Lett. **4**, 133, (1985).
[10] G. Girerd, P. Guiraldenq, N. Nu, Wear **102,** 233, (1985).
[11] B. Prakash, K. Hiratsuka, Tribol. Lett. **8,** 153, (2000).
[12] K. Hiratsuka, S. Norose, T. Sasada, B. Prakash, N. Takahashi, Proceedings of the 29th Japan Congress

on Material Research, 105, (1986).
[13] G. Li, Y.Q. Wang, L.M. Wang, Y.P. Gao, R.J. Zhang, Z.J. Zhan, L.L. Sun, J. Zhang, W.K. Wang, J. Mater. Res.**17,** 1877, (2002).
[14] T. Gloriant, J. Non-Cryst. Solids **316,** 96, (2003).
[15] M. Anis, W.M. Rainforth, H.A. Davies, Wear **172,** 135, (1994).
[16] P.J. Blau, Wear **205,** 431, (2001).
[17] J.A. Garcia, M. Rivas, M. Tejedor, A. Svalov, A.R. Pierna, F.F. Marzo, J. Mag. Magnetic Mat**. 290,** 1499, (2005).
[18] K. Mohri, A. Hernando, V. Madurga, M.C. Sanchez-Trujillo, M. Vazquez (Eds.), Magnetic Properties of Amorphous Metals, Elsevier, Amsterdam, 360, (1987).
[19] G. Herzer, H.R. Hilzinger, A. Hernando, V. Madurga, M.C. Sanchez-Trujillo, M. Vazquez (Eds.), Magnetic Properties of Amorphous Metals, Elsevier, Amsterdam 354, (1987).
[20] Amorphous Metals VITROVAC, Vacuumschmelze Catalogue, Edition 07, (1989).
[21] H. Chiriac, M. Lozovan, M. Neagu, Acta. Physica. Slovaca. **68,** 695, (1998).
[22] D. R. dos Santos, I. L. Torriani, F. C. S. Silva, M. Knobel, J. Appl. Phys, **86**, 6993, (1999).
[23] A. Hernandot, M. Vazquez, J. M. Barandiarans J. Phys. E: Sci. Instrum. **21,** 1129, (1988).
[24] S. Jana, U. Ramamurty, K. Chattopadhyay, Y. Kawamura, Mat. Sci. Eng.A **375,** 1199, (2004).
[25] U. Ramamurty, S. Jana, Y. Kawamura, K. Chattopadhyay Acta. Mater. **53,** 70, (2005).
[26] S. Jana, R. Bhowmick, Y. Kawamura, K. Chattopadhyay, U. Ramamurty Intermetallics **12,** 1097, (2004).
[27] H. Zhang, X. Jing, G. Subhash, L. J. Kecskes, R. J. Dowding Acta. Mater. **53,** 3849, (2005).
[28] F.Q. Yang, K. Geng, P.K. Liaw, GJ Fan, H Choo Acta. Mater. **55,** 321, (2007).
[29] Th.H.de Keljser, J. I. Langford, E.J.Mittemeijer , A. B. P.Vogels J. Appl. Cryst. **15,** 308, (1982).
[30] T.P.Yadav, N.K. Mukhopadhyay, R.S. Tiwari, O.N. Srivastava, Mat. Sci. Eng. A **393,** 366, (2005).
[31] A. Leonhard, L.Q. Xing, M. Heilmaier, A. Gebert, J. Eckert, L.Schultz, Nanostruct. Mater. **10,** 805, (1998).
[32] L.Q. Xing, J. Eckert, L. Schultz, Nanostruct. Mater. **12,** 503 (1999).

*Corresponding author: kedarbhp@rediffmail.com